Cell boundary detection for quantitative studies of the role of tetraspanin CD82 in cell-cell adhesion

Stroe, Paul; Claridge, Ela; Odintsova, Elena

DOI:
10.1016/j.procs.2016.07.031

Document Version
Publisher's PDF, also known as Version of record

Citation for published version (Harvard):
Stroe, P, Claridge, E & Odintsova, E 2016, Cell boundary detection for quantitative studies of the role of tetraspanin CD82 in cell-cell adhesion. in *Procedia Computer Science: Proceedings of Medical Image Understanding and Analysis Conference (MIUA 2016).* Procedia Computer Science, vol. 90, Elsevier, pp. 107–112, Medical Image Understanding and Analysis Conference (MIUA 2016), Loughborough, United Kingdom, 6/07/16. https://doi.org/10.1016/j.procs.2016.07.031

Available online at www.sciencedirect.com

ScienceDirect

Procedia Computer Science 90 (2016) 107 – 112

Procedia Computer Science

International Conference On Medical Imaging Understanding and Analysis 2016, MIUA 2016, 6-8 July 2016, Loughborough, UK

Cell boundary detection for quantitative studies of the role of tetraspanin CD82 in cell-cell adhesion

Paul Stroe[a], Ela Claridge[a]*, Elena Odintsova[b]

[a]*School of Computer Science, University of Birmingham, Birmingham B15 2TT, U.K.*
[b]*Institute of Cancer and Genomic Sciences, University of Birmingham, Birmingham B15 2TT, U.K.*

Abstract

Cell-cell adhesion is mediated by interaction of a number of protein complexes residing on the cell plasma membranes. Disruption of these complexes affects structural and functional integrity of tissues. It has been hypothesized that a membrane protein tetraspanin CD82, a known metastasis suppressor, may play a role in regulating cell adhesion. Two proteins of interest (PG and Dsg2) have been fluorescently tagged in cells expressing CD82 and in control cells, and imaged over the course of three hours. This paper describes a fully automatic method for quantitative analysis of PG and Dsg2 fluorescence. Cell boundaries are detected by the application of second-order steerable Gaussian filters. Cells are then segmented by closing the detected boundaries. Fluorescence levels are computed from a region lying around ± 1.5 microns from the centre-line between adjacent cells. Mean fluorescence levels obtained for thirty three cell images show that both the levels and the dynamics are different between the control and the CD82-expressing cells, which suggests that CD82 may play a role in cell-cell adhesion.

Peer-review under responsibility of the Organizing Committee of MIUA 2016

Keywords: Cell segmentation; Steerable Gaussian filters; Fluorescence microscopy; Quantitative analysis; Cell-cell adhesion; Tetraspanin CD82.

1. Introduction

Tissue integrity in multicellular organisms is maintained through intercellular cell junctions, including *adherens junctions* and *desmosomes*. The junctions consist of adhesive protein complexes which not only facilitate cell-cell adhesion but also regulate such important processes as epithelial morphogenesis, differentiation and wound

* Corresponding author. *E-mail address:* e.claridge@cs.bham.ac.uk

Peer-review under responsibility of the Organizing Committee of MIUA 2016
doi:10.1016/j.procs.2016.07.031

healing[1-2]. Compromised function of desmosomes, either due to mutation or loss, leads to various human diseases, including cancer[3]. Two proteins of interest in this study are desmoglein 2 (Dsg2), a desmosomal transmembrane protein, and plakoglobin (PG), a protein which is a component of desmosome and in steady state conditions is mainly localised on the plasma membrane. Preliminary experiments carried out at the Institute of Cancer and Genomic Sciences, University of Birmingham, suggested that the desmosomal adhesion might be regulated by a membrane protein, tetraspanin CD82, which is a known metastasis suppressor. The aim of the current study was to examine the nature of potential interactions between CD82 and desmosomal proteins PG and Dsg2. The effect of CD82 was studied in the cells which were genetically modified to overexpress CD82. The assembly/disassembly of desmosomal complexes was induced by changing Ca^{2+} concentration in growth media. This involved tagging PG and Dsg2 with different fluorescent markers and investigating their dynamic changes over the course of time. In images acquired using confocal fluorescence microscope pixel brightness is a measure of the abundance of a marker, and hence a protein. The laboratory staff carried out analysis semi-manually by outlining several cell boundaries in a small number of randomly selected image areas and measuring their mean pixel intensity. Such methods are slow and laborious, and statistical results may not be reliable due to a small amount of data collected in this way. This paper describes a fully automatic method for collecting the required information and presents a preliminary observations regarding the role of CD82 in regulation of desmosomal function.

2. Materials and methods

2.1. Cell preparation and imaging

The cell imaging experiments used the breast cancer cell line MCF7 stably transfected with CD82 (MCF7-CD82) and control cells (MCF7-puro)[4]. Cells were plated on Lab-Tech chambered coverglass and allowed to spread and form a monlayer. After 48 hours the medium on cells was changed for Ca^{2+} -free. The cells were fixed with ice-cold methanol for 10 min at -20^{o}C following 1, 2 and 3 hour incubation. Two wells were fixed before medium change and used as a control. Following fixation the cells were stained with primary antibodies against PG and Dsg2, and co-stained with the appropriate secondary antibodies conjugated to Alexa Fluor fluorophores (green - AF488, AF568 - red, respectively). Confocal images (RGB, 512x512 pixels) were acquired with a Zeiss LSM 510 confocal laser scanning system using Plan-Apochromat 63x/1.4 oil immersion objectives. Images used for quantification were taken using the same gain and offset settings. This study utilized 66 images (33 stained for PG and 33 stained for Dsg2), as detailed in Table 1. Eight were used in the algorithm development (3 for training and parameter optimisation and 5, unseen, for evaluation). All the images were used the analysis of dynamic changes in the levels of PG and Dsg2.

Table 1. Images used for computing the levels of PG and Dsg2 over the course of time.

Cell line	Time course	Number of images
MCF7-puro	before Ca^{2+} switch	5
	1 hour after switch	5
	2 hours after switch	3
	3 hours after switch	5
MCF7-CD82	before Ca^{2+} switch	4
	1 hour after switch	4
	2 hours after switch	3
	3 hours after switch	4

2.2. Image analysis

The objective of image analysis is to extract quantitative information about levels of PG and Dsg2 at cell boundaries (cell-cell contacts). This required the detection of the boundaries followed by computation of mean image intensities in green-tagged (PG) and red-tagged (CD82) fluorescence images. The development was carried out on the training set, evaluation used the test set, and quantitative results were computed for all the images.

Boundary detection. Boundary detection was carried out on the green channel (PG) images. PG is mainly localized at the plasma membrane and as such should clearly demarcate cell boundaries. However, the green fluorophore were also present at varying levels throughout the image, possibly due to disassembly of desmosomes following the Ca^{2+} removal and movement of disassembled parts of adhesion structures towards the cell interior. Simple methods such as thresholding or the application of edge detection operators were unsuitable as they provided many false positives away from the cell boundaries. These methods did not work because their responses were too local and isotropic, not distinguishing between small speckles and elongated linear structures corresponding to true boundaries. The solution adopted was to use second-order steerable Gaussian filters[5]. These are narrow, orientation selective convolution filters, defined by their direction (θ) and two Gaussian spread parameters σ_1 and σ_2 (see Figure 1). Filter F_θ integrates responses along its major axis and its orthogonal neighbourhood as well as smoothing out any isolated speckles. A single application of a filter F_θ will preferentially detect features aligned in direction θ. Taking a pixel-wise maximum over all the filtered images results in a single image I_b showing the detected boundary responses.

$$I_b = \max_\theta F_\theta$$

Through experimentation θ was set to 30°, resulting in six directional images, σ_1 and σ_2 were set to 7. Implementation was based on a Matlab filexchange function[6].

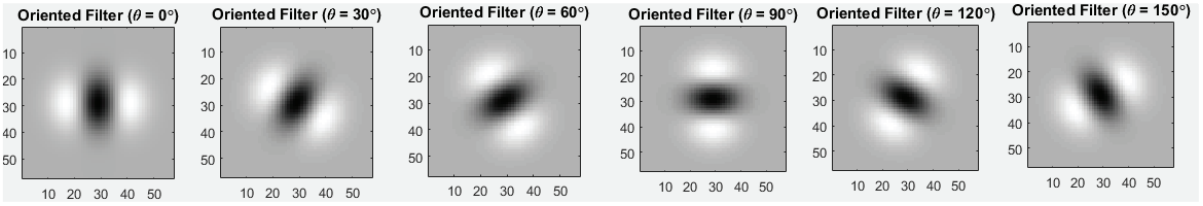

Fig. 1. Steerable Gaussian Filters at different angles where Θ denotes the angle

Quantification of fluorescence levels. In the investigation concerning cell adhesion the most relevant region lies around ± 1.5 microns from the centre-line between adjacent cells. The centre-lines were detected by, first, thresholding the boundary response image I_b and then morphological thinning (Matlab function `bwmorph`) of the resulting binary image and removing non-boundary segments. The threshold value was derived by the analysis of histograms in the training set. As they all had similar distribution, the same threshold was used consistently for all the image data. In the final step the centre-lines were expanded by dilation (Matlab function `imdilate`) to create a binary mask covering the boundary region of interest for the fluorescence quantification. Mean pixel values for this region were computed for both PG (green) and CD82 (red) fluorescence images. Figure 2 (next page) shows a sequence of images representing results of the processing pipeline.

Cell count. The parameter of the primary interest to bioscientists is the mean fluorescence level as a function of time. However, the mean fluorescence response per cell may convey additional information, and for this reason the cell count was implemented as an additional quantitative feature. With the cell boundaries detected it would be trivial to count the number of objects that the boundaries enclose. However, some of the enclosed regions represent intercellular spaces and should not be included in the count. Typically the real cells are larger than intercellular spaces. To arrive at a size threshold value all the intercellular spaces in the training dataset were identified by hand

and their maximum taken as the threshold value. This threshold excluded also small incomplete cell fragments at the image borders which were not manually counted either. The mean fluorescence response per cell was computed as the total fluorescence divided by the number of valid cells in the image.

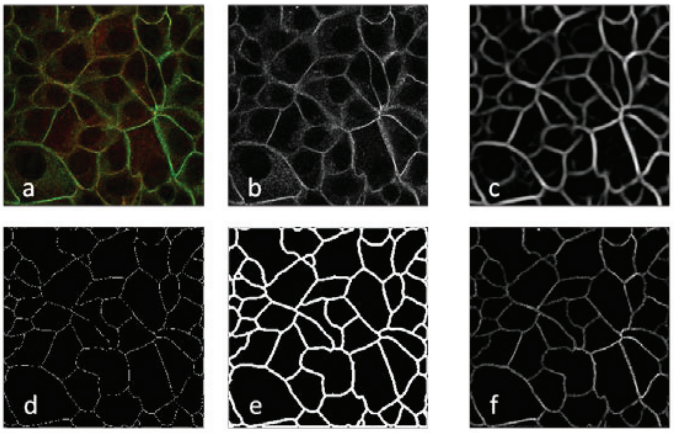

Fig. 2. (a) Original image; (b) Green plane extracted from (a) representing levels of green-tagged PG; (c) Ib - maximum over results of convolution of (b) with five steerable filters shown in Fig. 1; (d) Result of morphological thinning applied to (c); (e) Result of morphological dilation applied to (d); Levels of PG at cell boundaries represented as pixel brightness.

3. Evaluation

The parameters for the above processing pipeline were established using a training set of three images. Evaluation was performed on five unseen images. For the centre-line boundary detection, as the ground truth in the form of hand-outlined cells was not available, a simple scheme for computing sensitivity of detection was employed. True positive value was taken to be the combined length (in pixels) of the boundary lines detected by the method that coincided with the actual boundary. False negative value was taken to be the combined length of the boundary lines that were missed; these were inserted by hand. Figure 3 shows one of the images used for validation with the computer-detected boundaries shown in white and the missing boundaries shown in red. For the evaluation of cell count, the cell numbers returned by the computer method were compared to those manually counted. Table 2 summarises the results of evaluation.

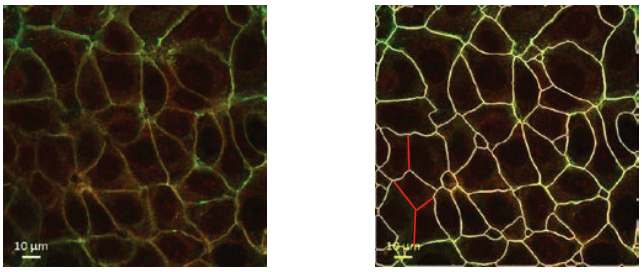

Fig. 3. Left: original image; Right: automatically detected boundaries (yellow) and missing boundaries (red).

Table 2. Evaluation of cell boundary detection and cell count. Results are shown for 5 unseen images in the test set.

Image	Missed	True Positive	False Negative	Sensitivity	Manual cell	Automatic	Percentage

	Edges			TP/(TP+FN)	count	cell count	correct
1	2	6873	37	0.99	42	39	93
2	4	9101	369	0.96	36	37	97
3	2	8663	61	0.99	31	32	98
4	3	8592	132	0.98	45	43	96
5	1	7206	88	0.98	42	44	95

4. Results

A biological question that stimulated the development of this method was whether, and in what way, tetraspanin CD82 affects the dynamics of desmosomal proteins PG and Dsg2 when the junctional adhesion is disrupted by removing Ca^{2+} from the environment. The levels of PG and Dsg2 were computed individually for each of the thirty three images acquired in the experiments described in 2.1. The mean level values were then computed for each of the eight image groups shown in Table 1. Plots in Figure 4 show the mean levels for MCF7-puro and MCF7-CD82 over the course of time and those in Figure 5 show the mean levels per cell.

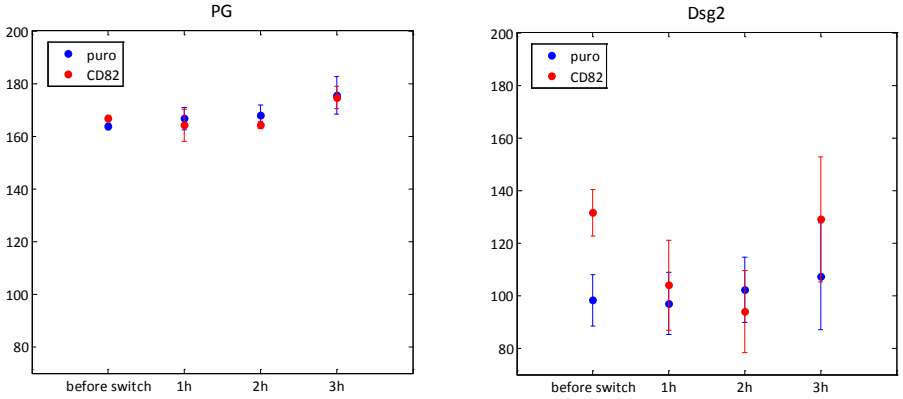

Fig. 4. Levels and time course of PG (left) and Dsg2 (right) in the breast cancer cell line MCF7. Blue dots: control cells (puro); red dots: cells stably transfected with CD82. X-axis: the time course [hours]; Y-axis: mean fluorescence level per image [A.U.].

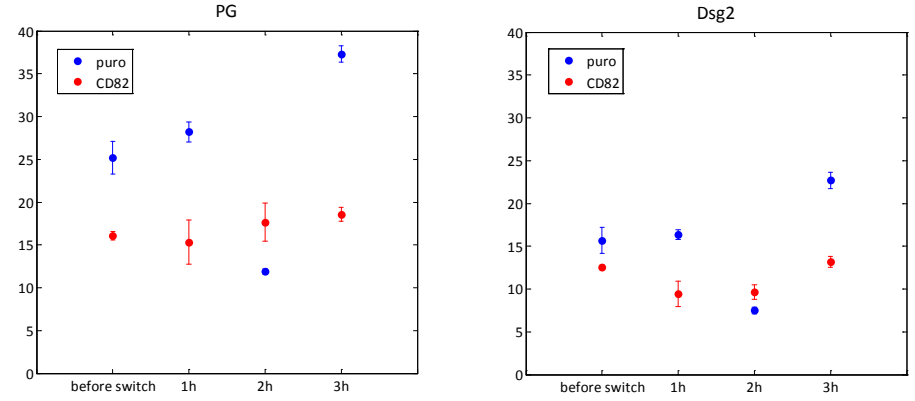

Fig. 5. Levels and time course of PG (left) and Dsg2 (right) in the breast cancer cell line MCF7. Blue dots: control cells (puro); red dots: cells stably transfected with CD82. X-axis: the time course [hours]; Y-axis: mean fluorescence level per cell [A.U.].

5. Discussion and conclusion

Biological studies clearly benefit from the ability to compute statistics over large image sets entirely without user intervention. In pilot experiments carried out manually by the laboratory staff it took 3 hours to derive similar statistics for four images. In contrast, using Matlab on a standard PC (Intel Core Quad CPU 2.33 GHz) the computations take approximately 3.8 sec per image (approximately 4 mins for the set of 66). Apart from removing subjectivity and tedium of the manual work, the ability to process large data sets improves reliability of such studies. Plots like those shown in Figures 4 and 5 aid the interpretation of biological phenomena. In this instance (Fig. 4) they suggest that PG dynamics over the course of three hours are not affected by the expression of CD82. On the other hand, CD82 expression seems to impact the dynamics of Dsg2. It can be seen that in the MCF7-puro (control) cells, Dsg2 levels remain relatively constant for 3 hours after Ca^{2+} removal. However, in MCF7-CD82 cells, the initial level of Dsg2 on the membrane is considerably higher, then drops in response to Ca^{2+} removal during the first two hours (even below the levels in control cells) after which it starts recovering. It can be seen that both the levels and the dynamics are different between the two cell lines which suggests that tetraspanin CD82 may play a role in cell-cell adhesion. This behaviour is consistent with the current understanding, however, to make firm conclusions from biological point of view the experiments will need to be repeated on more images for each condition and statistical analysis re-applied. The method described in this paper will make the process of analysis dependable and fast.

References

1. Green, K.J., Getsios, S., Troyanovsky, S. and Godsel, L.M., 2010. Intercellular junction assembly, dynamics, and homeostasis. Cold Spring Harbor perspectives in biology, 2(2), p.a000125.
2. Green, K.J. and Simpson, C.L., 2007. Desmosomes: new perspectives on a classic. Journal of Investigative Dermatology, 127(11), pp.2499-2515.
3. Dusek, R.L. and Attardi, L.D., 2011. Desmosomes: new perpetrators in tumour suppression. Nature Reviews Cancer, 11(5), pp.317-323.
4. Odintsova, E., Voortman, J., Gilbert, E. and Berditchevski, F., 2003. Tetraspanin CD82 regulates compartmentalisation and ligand-induced dimerization of EGFR. Journal of cell science, 116(22), pp.4557-4566.
5. Freeman, W.T. and Adelson, E.H., 1991. The design and use of steerable filters. IEEE Transactions on Pattern Analysis & Machine Intelligence, (9), pp.891-906. Vancouver
6. Jincheng Pang, Steerable Filter, January 2014. URL http://uk.mathworks.com/matlabcentral/fileexchange/44956-steerable-filter